Gradient Polarity Solvent Wash for Separation and Analysis of Electrolyte Decomposition Products on Electrode Surfaces

Journal of the Electrochemical Society, 2020 **167** 020506

Gradient Polarity Solvent Wash for Separation and Analysis of Electrolyte Decomposition Products on Electrode Surfaces

Chen Fang,[1,*] Zhimeng Liu,[1] Jonathan Lau,[1] Mahmoud Elzouka,[1] Guangzhao Zhang,[1] Piyachai Khomein,[1] Sean Lubner,[1] Philip N. Ross,[2] and Gao Liu[1,z]

[1]*Energy Storage and Distributed Resources Division, Lawrence Berkeley National Laboratory, Berkeley, California 94720, United States of America*
[2]*Materials Sciences Division, Lawrence Berkeley National Laboratory, Berkeley, California 94720, United States of America*

The solid electrolyte interphase (SEI) formed during the cycling of lithium-ion batteries (LIBs) by decomposition of electrolyte molecules has key impact on device performance. However, the detailed decomposition process and distribution of products remain a mystery due to the wide variety of electrochemical pathways and the lack of facile analytical methods for chemical characterization of SEIs. In this report, a gradient polarity solvent wash technique involving the use of solvents with gradually increased polarities is employed to sequentially remove different SEI components from electrode surfaces. Fourier transform infrared (FTIR) spectroscopy is utilized to characterize the SEI composition. The impacts of electrolyte additives and discharge rates over SEI formation are illustrated. This study presents a new concept of rationally controlled solvent wash technique for electrode surface analysis that can selectively remove targeted components. The findings in this study provide experimental support for the slow charge formation processes commonly employed for LIBs in industry.
 [DOI: 10.1149/1945-7111/ab6447]

Manuscript submitted August 30, 2019; revised manuscript received November 15, 2019. Published January 7, 2020. *This was Paper 323 presented at the Atlanta, Georgia, Meeting of the Society, October 13–17, 2019.*

Supplementary material for this article is available online

There has been an emerging demand for high-performance lithium-ion batteries (LIBs) to satisfy the rapidly growing global energy storage market for portable electronics and electric vehicles. Silicon is considered a promising anode material for next-generation LIBs because of its high theoretical capacity (4212 mAh $\cdot$ g^{-1}, as for fully lithiated alloy $Li_{22}Si_5$), which is over an order of magnitude higher than that of graphite currently used in commercial LIBs (372 mAh g^{-1}).[1,2] A major challenge for improvement of silicon-based LIBs is to rationally control the electrochemical decomposition of the electrolyte components and thus the formation of protective solid electrolyte interphase (SEI) on silicon.[3,4] SEIs are thin, passivating films on electrode surfaces that allow diffusion of Li^+ but prevent undesired parasitic reactions with the solvent molecules that negatively affect the device performance. The use of a small amount of additive is a cost-efficient approach for tuning the electrochemical properties of electrolyte systems without altering the skeletal composition or fabrication process of LIBs.[3,5,6] Additives are often incorporated as sacrificial components for SEI formation, and can have key impacts on battery's performance.[7–13]

In order to gain a deeper understanding of the properties of SEIs, it is crucial to develop facile SEI analytical methods. Conventional ex situ analytical methods such as X-ray photoelectron spectroscopy (XPS) are not convenient for in-depth characterizations of SEIs and near SEIs.[14,15] Washing electrodes with electrolyte solvents is a common practice for measurement of the inner SEI sections.[16–19] Such rinsing has also been utilized to remove the organic upper layers from the inorganic bottom layers for in-depth analysis.[20–22] To the best of our knowledge, there have been few reports attempting to develop advanced washing protocols.[22–24] The common washing techniques have been shown to possibly interfere with SEIs.[25,26] It is desirable to develop more sophisticated washing strategies to resolve SEIs.[27] Fourier transform infrared spectroscopy (FTIR) can analyze key organic components[28] used in lithium sulfur batteries.[29] FTIR has also been widely employed for characterization of LIB electrodes of silicon[15,30,31], graphite[24,32–38], and metal[27,39] materials. FTIR is a facile analytical tool that is suitable for electrode surface characterization when combined with well-controlled electrode washing.

In this work, we utilize gradient polarity solvent wash (gradient wash) technique to examine the SEIs and near SEIs produced by polar and non-polar methacrylate additives under a series of electrochemical conditions. Copper (Cu) and silicon (Si) electrodes were electrochemically cycled with $LiPF_6$ ethylene carbonate/ethyl methyl carbonate (EC/EMC) electrolyte containing methacrylate additives to reveal additives' impacts on SEIs. With a binary, polarity-tunable solvent system, it was possible to selectively remove different SEI components by successive washing steps to realize precise SEI characterization. The electrode surfaces before and after each wash were analyzed with FTIR.

Experimental

Material preparation.—Copper (Cu) foil electrodes (5/8 inch) were thoroughly washed with ethanol and dried under vacuum before use. Silicon (Si) electrodes (500 nm thick Si film sputtered on Cu foil electrodes, 1/2 inch) were supplied by Oak Ridge National Laboratory and used as received. 1.2 M $LiPF_6$ EC/EMC (3:7 w/w, Tomiyama Pure Chemical Industries, LTD) was used as the base electrolyte. Additive-containing electrolytes (5 wt% for Cu electrodes, 2 wt% for Si electrodes) with lauryl methacrylate (Acros) or triethylene glycol methyl ether methacrylate (Sigma Aldrich) were used for comparison. For synthesis of standard polymers of methacrylate additives, a solution of 3 ml dimethylformamide containing 0.5 g methacrylate and 0.5 mg azobisisobutyronitrile was heated at 80 degree Celsius under N_2 atmosphere for 12 h, after which, the polymers were obtained and purified by three dissolve-precipitate cycles in ether.

Cell fabrication and electrochemical testing.—The 2325 coin cells (National Research Council, Canada) were assembled with Cu or Si electrodes in a glovebox (<0.5 ppm O_2 and H_2O) using Celgard 2400 separators (Celgard) against lithium foil (Albemarle) counter electrode. Electrochemical testing of the assembled cells was performed with Maccor Series 4000 Battery Test system at 30 °C. For SEI formation, Cu electrodes were discharged vs Li metal anodes using linear sweep voltammetry technique from the

*Electrochemical Society Member.
[z]E-mail: gliu@lbl.gov

open-circuit voltage (OCV) to 50 mV vs Li/Li^+ at 1 or 0.167 mV s^{-1} (60 or 10 mV min^{-1}), at which point the voltage was held at 50 mV for 2 h. Slower formation cycles utilized a sweep rate of 0.0167 mV s^{-1} (1 mV min^{-1}) from OCV to 50 mV vs Li/Li^+ at which point the voltage was held for 48 h. Si electrodes were discharged in a similar manner at 0.167 mV s^{-1} (10 mV min^{-1}) until 50 mV vs Li/Li^+ and held at 50 mV for 2 h, but were then charged to 1 V at the same rate for delithiation. The processed electrodes were carefully removed from the cells in glovebox and dried under vacuum for 12 h.

Gradient polarity solvent wash and FTIR.—The gradient polarity solvent wash of electrodes was performed in glass vials, where the electrodes were immersed under 5 ml solvents with gentle manual agitation for 30 s. The washing steps were carried out immediately after each FTIR experiment to minimize air exposure of the electrode samples. The solvents used were 0% to 100% volume ratio ethyl acetate (EA) in hexane (Hex) solutions with 10-percent intervals (i.e. 0%, 10%, 20%, 30% EA/Hex, etc). After rinsing, the electrodes were immediately dried and stored under vacuum until characterization. The FTIR measurements were conducted on a Thermo Nicolet iS50 FTIR spectrometer with a reflective accessory. The spectra were collected with 4 cm^{-1} resolution averaged over 32 scans. For each FTIR experiment, the samples were measured without delay. These procedures were taken to minimize air exposure and to maintain consistence of air exposure time across different samples, which could cause slight shift of FTIR peak positions.

Results and Discussion

In order to accurately control the discharge process of Cu electrodes, linear sweep voltammetry was performed from OCV to 50 mV vs Li/Li^+ for formation of SEIs, followed by a voltage-constant discharge step till the current fell to the baseline. A non-polar additive, lauryl methacrylate (LMA), and a polar additive, triethylene glycol methyl ether methacrylate (TEGMA), were individually added to the $LiPF_6$ EC/EMC base electrolyte to examine their impacts on SEI formation. Gradient wash was carried out with ethyl acetate (EA) and hexane (Hex) mixed solvents of gradually increased EA ratios. FTIR measurements were performed to chemically analyze the SEIs before and after each wash.

Gradient wash and FTIR for Cu electrodes cycled at slow discharge rate.—First, gradient wash was applied to the Cu electrode cycled with the base electrolyte at 0.0167 mV s^{-1} (1 mV min^{-1}) scan rate (Fig. 1a, S1a is available online at stacks.iop.org/JES/167/020506/mmedia). The unwashed electrode surface (Spectrum I) presented peaks at 1801, 1773, 1189, 1076, 825 cm^{-1}, corresponding to residue EC:$LiPF_6$ solvate.[27] In addition, EMC:$LiPF_6$ solvate[40] (1260, 1019, 874 cm^{-1}) and Li_2CO_3[41] (1508 and 1420 cm^{-1}) were observed. The set of peaks at 1639, 1404, 1312 cm^{-1} agree with lithium ethylene di-carbonate (LEDC)[27] or lithium ethylene mono-carbonate (LEMC)[42] (cannot distinguish with ex situ FTIR in this study, thus not discussed separately). On the other hand, the strong intensity and broadness of the 1639 cm^{-1} peak indicate that it is an overlapped peak with $LiHCO_3$.[43] The formation of $LiHCO_3$ was likely due to the exposure of lithium salts to CO_2 in the air. Other possible EC decomposition products diethyl 2,5-dioxahexane dicarboxylate (DEDOHC) and polyethylene carbonate (poly-EC)[44] could not be confirmed or excluded due to the lack of unique characteristic peaks. This electrode surface film was gradually washed off by 0%–30% EA/Hex (Spectrum II–IV). No outstanding FTIR signal was detected after each wash of 40%–100% EA/Hex.

The presence of LMA and TEGMA additives in the electrolyte delivered disparately different results as they could polymerize on electrode surfaces. As observed from the unwashed electrode, LMA formed a robust poly-LMA layer on Cu surface (Fig. 1b Spectrum I, Fig. S1b), which was confirmed with the synthetic poly-LMA sample (Spectrum IV, 2920, 2850, 1725, 1461, 1263, 1243 and 1145 cm^{-1}). It is worth noting that the poly-LMA layer significantly altered the electrode surface properties and thus the behavior of electrolyte molecules on Cu surface. Poly-LMA has rich content of dodecyl ($C_{12}H_{25}$) moieties, which renders the electrode surface rather non-polar. The commonly expected adsorption of electrolyte molecules onto the electrode surface was consequently rejected by this hydrocarbon-rich Cu electrode surface, as evidenced by the absence of characteristic peaks for EC, EMC and $LiPF_6$. The initial hexane wash significantly reduced the intensity of poly-LMA peaks (Spectrum II), possibly because the low-mass polymers were rinsed off. Despite intensity decrease, the characteristic peaks for methylene (2920, 2850 cm^{-1}) and carbonyl (1725 cm^{-1}) groups persisted throughout all gradient washes (Spectrum III, Fig. S1b), indicating the formation of a dense poly-LMA passivation film.

TEGMA additive also produced a poly-TEGMA film on Cu surface (Fig. 1c, Spectrum I), which, due to its high polarity, did not resist adsorption of electrolyte (EC/EMC:$LiPF_6$, 1809, 1780, 1269, 1196, 1082, 1025, 833 cm^{-1}), $LiHCO_3$ (1623 cm^{-1}) and Li_2CO_3 (1510, 1419 cm^{-1}). The poly-TEGMA layer was fully exposed after gradient wash with 0%–30% EA/Hex solutions (Fig. 1c, Spectrum II). This polar polymer film survived all remaining washing steps with 40%–100% EA/Hex (Spectrum III, Fig. S1c). Its chemical composition was confirmed by comparison with the synthetic sample (Spectrum IV, 1726, 1455, 1112 cm^{-1}). The removal of dried electrolyte with 0%–30% EA/Hex is consistent with the case of the base electrolyte. It is worth noting that the carbonyl peak for poly-TEGMA at 1726 cm^{-1} presented a red shift before removal of lithium salt species (Spectrum II, III) due to solvation effect.[44]

Gradient wash and FTIR for Cu electrodes cycled at fast discharge rates.—The impact of discharge rate on SEI formation was evaluated using samples cycled at 0.167 and 1 mV s^{-1} (10 and 60 mV min^{-1}). It is worth noting here that the success of gradient polarity solvent wash for SEI analysis was fully demonstrated with the cells scanned at 0.167 mV s^{-1} (10 mV min^{-1}) as described in the following paragraphs. The complete set of FTIR spectra are shown in Figs. S2 and S3.

The scan rate of 0.167 mV s^{-1} (10 mV min^{-1}) was tested first. Before gradient wash, the Cu electrode cycled with base electrolyte presented EC:$LiPF_6$ solvate (1803, 1770, 1196, 1081, 884 cm^{-1}), LEDC/LEMC (1408, 1312 cm^{-1}) and $LiHCO_3$ (1639 cm^{-1}) as shown in Fig. 2a, Spectrum I. These species were completely removed by 0%–30% EA/Hex gradient wash (Spectrum II–IV), which is consistent with the previous cases. However, under this faster scan rate, Li_2CO_3 was not observed. Li_2CO_3 is considered as an electrolyte decomposition product during late-stage SEI evolution and battery cycling.[3] Therefore, the absence of Li_2CO_3 product under this faster scan rate is due to the limited electrochemical reaction time.

With the LMA additive, the unwashed Cu electrode presented poly-LMA (Fig. 2b, Spectrum I) as confirmed with the synthetic sample (Spectrum IV). $LiHCO_3$ (1638 cm^{-1}) and $LiPF_6$ (832 cm^{-1}) were observed as well, but no Li_2CO_3 or LEDC/LEMC was found. The poly-LMA species were immediately washed off by hexane (Fig. S2b), possibly because only low-mass polymers were produced at this faster scan rate. The remaining peaks at 1561, 1285, 843 cm^{-1} after gradient wash (Spectrum II–III) are attributed to lithium methacrylate[45,46], which could originate from LMA decomposition.

The effectiveness of gradient polarity solvent wash for sequential removal of different chemical species was fully demonstrated with the Cu electrode cycled at 0.167 mV s^{-1} (10 mV min^{-1}) with TEGMA additive (Fig. 2c, S2c). Before wash, the Cu surface was covered with EC:$LiPF_6$ solvate and $LiHCO_3$ (no Li_2CO_3 or LEDC/LEMC). The residue EC was firstly removed by 0%–20% EA/Hex washes (Spectrum I vs II, disappearance of 1802, 1776, 1482, 1410, 1198, 1079 cm^{-1} peaks); then, $LiHCO_3$ (1639 cm^{-1}) was rinsed off by 30%–50% EA/Hex washes (Spectrum III, Fig. S2c); finally, $LiPF_6$ (833 cm^{-1}) was washed away by 30%–100% EA/Hex washes (Spectrum IV), fully exposing the underlying poly-TEGMA film (as

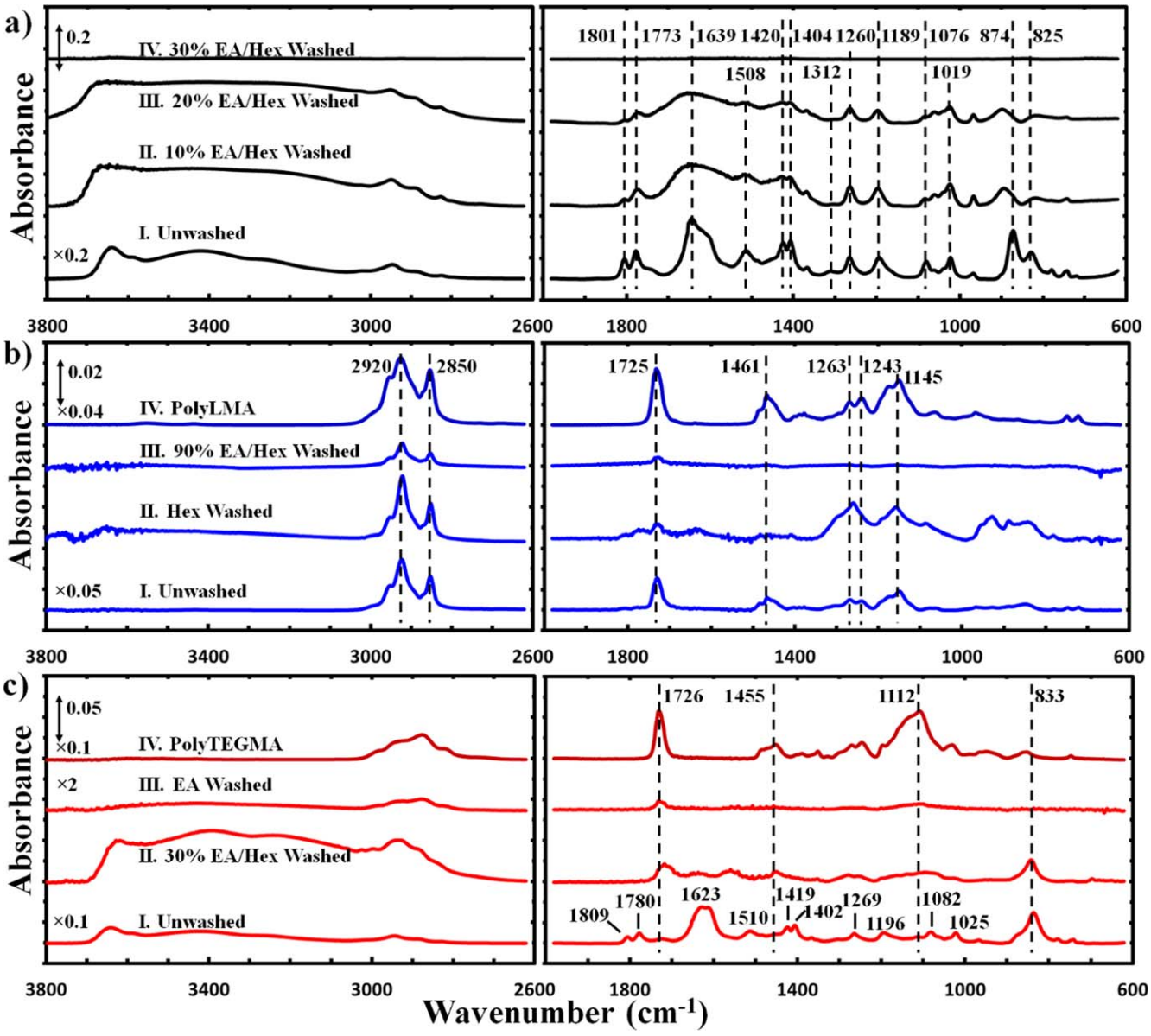

Figure 1. Selected FTIR spectra of unwashed and washed Cu electrodes cycled at 0.0167 mV s^{-1} (1 mV min^{-1}) rate with (a) no additive, (b) LMA additive and (c) TEGMA additive.

confirmed with synthetic sample, Spectrum V) with additive decomposition product lithium methacrylate (1563 cm^{-1}). Red shift of the carbonyl peak of poly-TEGMA before removal of lithium salts was observed in this case as well.

The highest 1 mV s^{-1} (60 mV min^{-1}) sweep rate led to more extensive electrolyte adsorption with no outstanding evidence for solvent molecule decomposition. The unwashed surface of the Cu electrode cycled with base electrolyte (Fig. 3a, Spectrum I) presented strong peaks for EC:$LiPF_6$ (1801, 1769, 1482, 1405, 1197, 1084, and 831 cm^{-1}) and $LiHCO_3$ (1641 cm^{-1}). Like the previous cases, these species were also rinsed off with 0%–30% EA/Hex (Spectrum II–IV), showing that the washing process was polarity-controlled rather than sample-specific.

As for the Cu electrode cycled with LMA additive (Fig. 3b), similar strong adsorption of EC:$LiPF_6$ (Spectrum I, 1803, 1763, 1486, 1404, 1193, 1078, and 837 cm^{-1}) with $LiHCO_3$ (1630 cm^{-1}) was observed for the unwashed surface. The peaks of LMA species seem to be in good agreement with the synthetic poly-LMA sample (Spectrum IV), but the extra characteristic peak for =C–H at 3004 cm^{-1} indicates that the residue LMA largely existed in the monomer form. Without the presence of a non-polar, electrolyte-repulsive poly-LMA film, strong adsorption of electrolyte molecules thus occurred on Cu surface, which were quickly rinsed off with gradient wash (Spectrum II–III).

On the other hand, TEGMA was still able to polymerize on Cu surface at this high scan rate. The unwashed Cu surface was found to be mainly covered with dried electrolyte (EC:$LiPF_6$, Fig. 3c, Spectrum I) while the gradient wash could sequentially wash off EC (1805, 1778 1481, 1401, 1187, 1088 cm^{-1}), $LiHCO_3$ (1630 cm^{-1}) and $LiPF_6$ (840 cm^{-1}), exposing the underlying poly-TEGMA layer (Spectrum II, III vs IV). The red shift of carbonyl group by solvation effect of lithium salt was still observed in this case.

Impact of discharge rate on reactions at Cu electrode surface.—The electrochemical treatment of Cu electrodes was carried out in a two-step manner, a linear sweep voltammetry (scan) step and a voltage-constant discharge (hold) step. The integrated charge consumption of the two steps can be used for rough approximation of the electrochemical reactions present in the cells (Fig. 4). For the

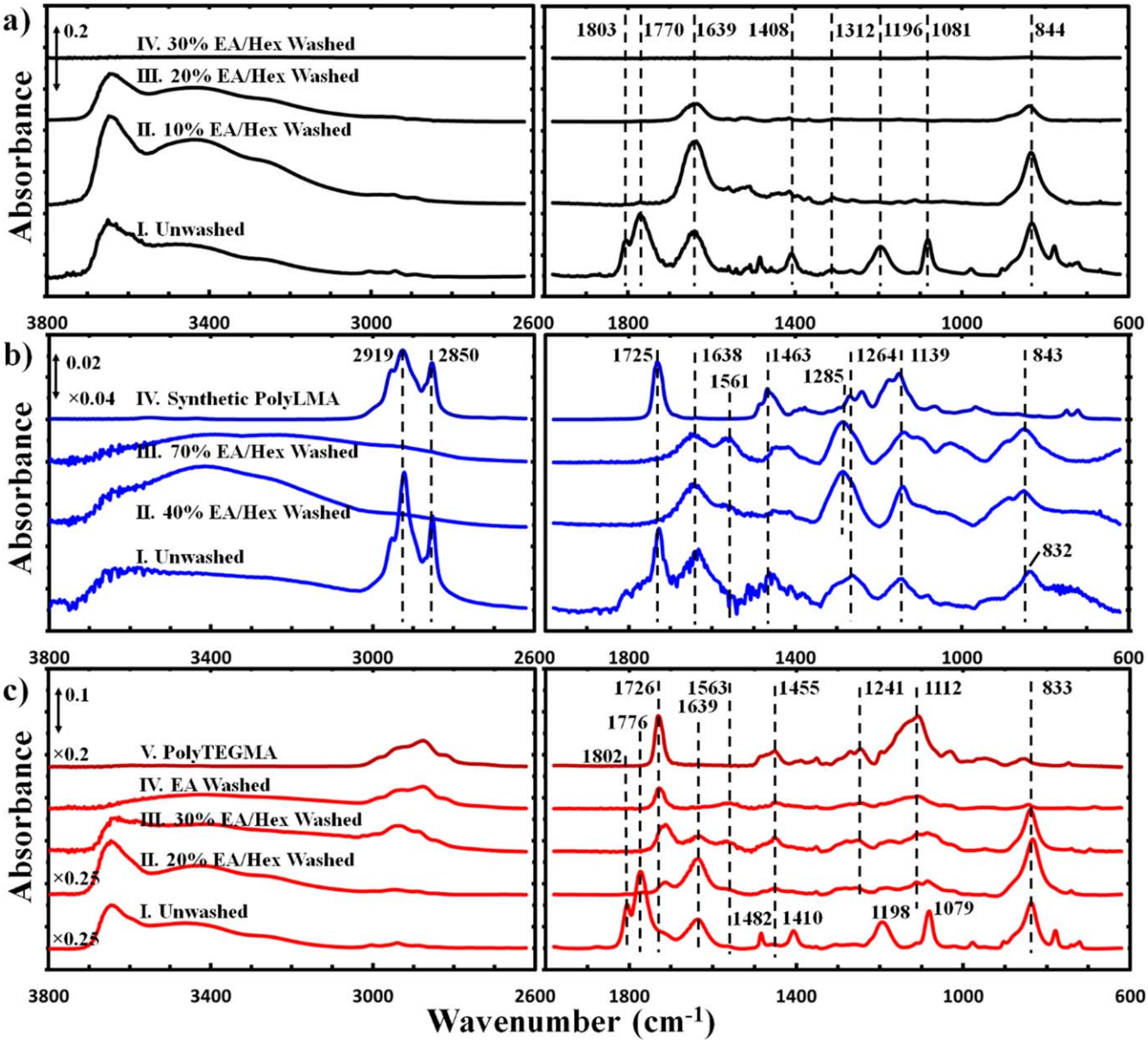

Figure 2. Selected FTIR spectra of unwashed and washed Cu electrodes cycled at 0.167 mV s^{-1} (10 mV min^{-1}) rate with (a) no additive, (b) LMA additive and (c) TEGMA additive.

scan steps at all rates, cells with additives showed higher charge consumption due to the extra polymerization reaction. LMA led to lower charge consumption than TEGMA because the non-polar LMA species on electrodes suppressed further additive reaction by repulsing the bulk electrolyte. For the hold steps after the slowest scan steps at 0.0167 mV s^{-1} (1 mV min^{-1}), the three different electrolytes had almost identical charge consumption (Fig. 4, left). This is because the formation of dense SEIs on the electrodes could effectively prevent further reactions in all three cases. On the other hand, faster scan rates at 0.167 mV s^{-1} (10 mV min^{-1}) could not lead to generation of strong passivation layers, thus the continuing reaction of TEGMA led to higher charge consumption during its hold step (Fig. 4, middle). This effect is more obvious in the case of the fastest scan rate at 1 mV s^{-1} (60 mV min^{-1}) as shown in Fig. 4, right section.

Gradient wash and FTIR for Si electrodes.—In addition to Cu electrodes, Si electrodes were also examined with gradient wash technique (Fig. 5, S4). The unwashed surface of the Si electrode cycled with base electrolyte (Fig. 5a) presented EC:$LiPF_6$ solvate (Spectrum I, 1807, 1767, 1405, 1204, 1081, 832 cm^{-1}) and LEDC[27,30]/LEMC[42] (1626, 1317 cm^{-1}), which were gradually washed off (Spectrum II–III) to leave Li_2CO_3[23,41] (1508, 1435 cm^{-1}) and $LiHCO_3$ (1614 cm^{-1}) on the surface. The peaks in the 800–1250 cm^{-1} region (Spectrum IV) after complete washing protocols are associated with lithium silicon oxide species.[47]

The Si electrode electrochemically treated with LMA additive presented poly-LMA (confirmed with synthetic sample, Spectrum IV), LEDC/LEMC (1645, 1400, 1308 1070 cm^{-1}) and $LiPF_6$ (835 cm^{-1}) as shown in Fig. 5b, Spectrum I. These species were gradually washed off (Spectrum II–III, Fig. S4b) as well to leave a broad peak at 1433 cm^{-1}, which is attributed to a mixture of carboxylate salts and Li_2CO_3.[47,48] No significant electrolyte adsorption was observed.

The TEGMA additive also resulted in formation of poly-TEGMA (Fig. 5c) on Si electrode. The unwashed Si surface presented EC:$LiPF_6$ (Spectrum I, 1802, 1771, 1406, 1188, 1084, 858 cm^{-1}) and LEDC/LEMC (1632, 1316 cm^{-1}), which were gradually washed off to expose the poly-TEGMA film beneath (Spectrum II, Fig. S4c),

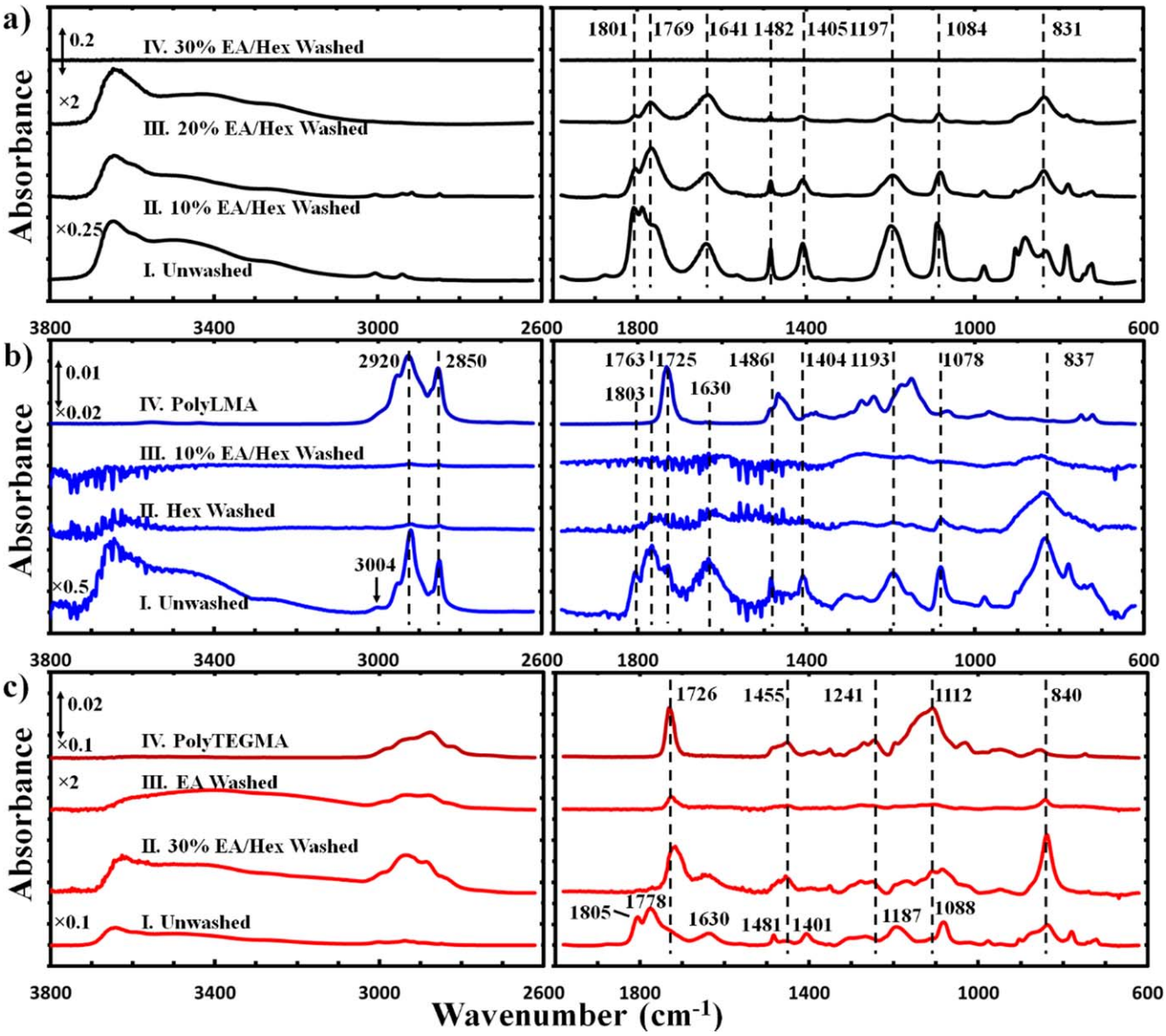

Figure 3. Selected FTIR spectra of unwashed and washed Cu electrodes cycled at 1 mV s^{-1} (60 mV min^{-1}) rate with (a) no additive, (b) LMA additive and (c) TEGMA additive.

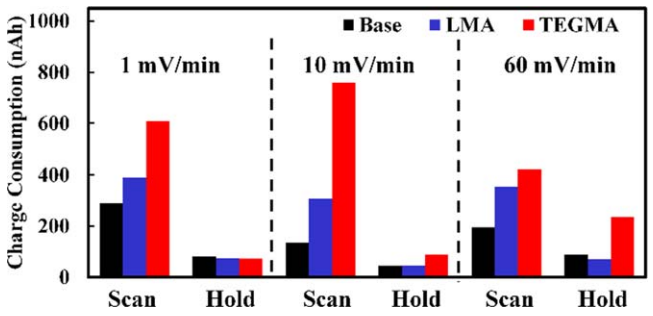

Figure 4. Charge consumption profile of cells containing base, LMA and TEGMA electrolytes cycled at different scan rates.

as confirmed with synthetic sample (Spectrum IV). After washing procedures, $LiHCO_3$ (1601 cm^{-1}) and Li_2CO_3 (1502, 1454 cm^{-1}) could be identified unambiguously (Spectrum III).

It should be noted that Si electrodes were treated with much less additives than Cu electrodes (so as to not interfere with regular Si surface chemistry), and thus the FTIR signals of the additive polymers may be hindered by the salts that prevailed the Si surface. This rationale is supported by the observation that the Si electrode cycled with LMA presented minor amount of dried electrolyte, which could only be repelled by the non-polar poly-LMA film. Overall, the electrochemical decomposition products on Si surfaces were found to be similar to those on Cu surfaces.

Conclusion

In summary, the decomposition products of $LiPF_6$ EC/EMC electrolyte with methacrylate additives were examined by FTIR using a gradient polarity solvent wash technique. The discharge rate has major impact on the electrolyte decomposition products on Cu electrode surfaces. With the base electrolyte that contains no additive, a slow scan rate of 0.0167 mV s^{-1} (1 mV min^{-1}) produced Li_2CO_3 and LEDC/LEMC while a faster scan rate at 0.167 mV s^{-1} (10 mV min^{-1}) yielded LEDC/LEMC but no Li_2CO_3. This is because the decomposition of electrolyte molecules to the final product Li_2CO_3 requires extended time, namely slow scan rate. The fastest scan rate at 1 mV s^{-1} (60 mV min^{-1}) resulted in no observable electrolyte decomposition. On the other hand, the

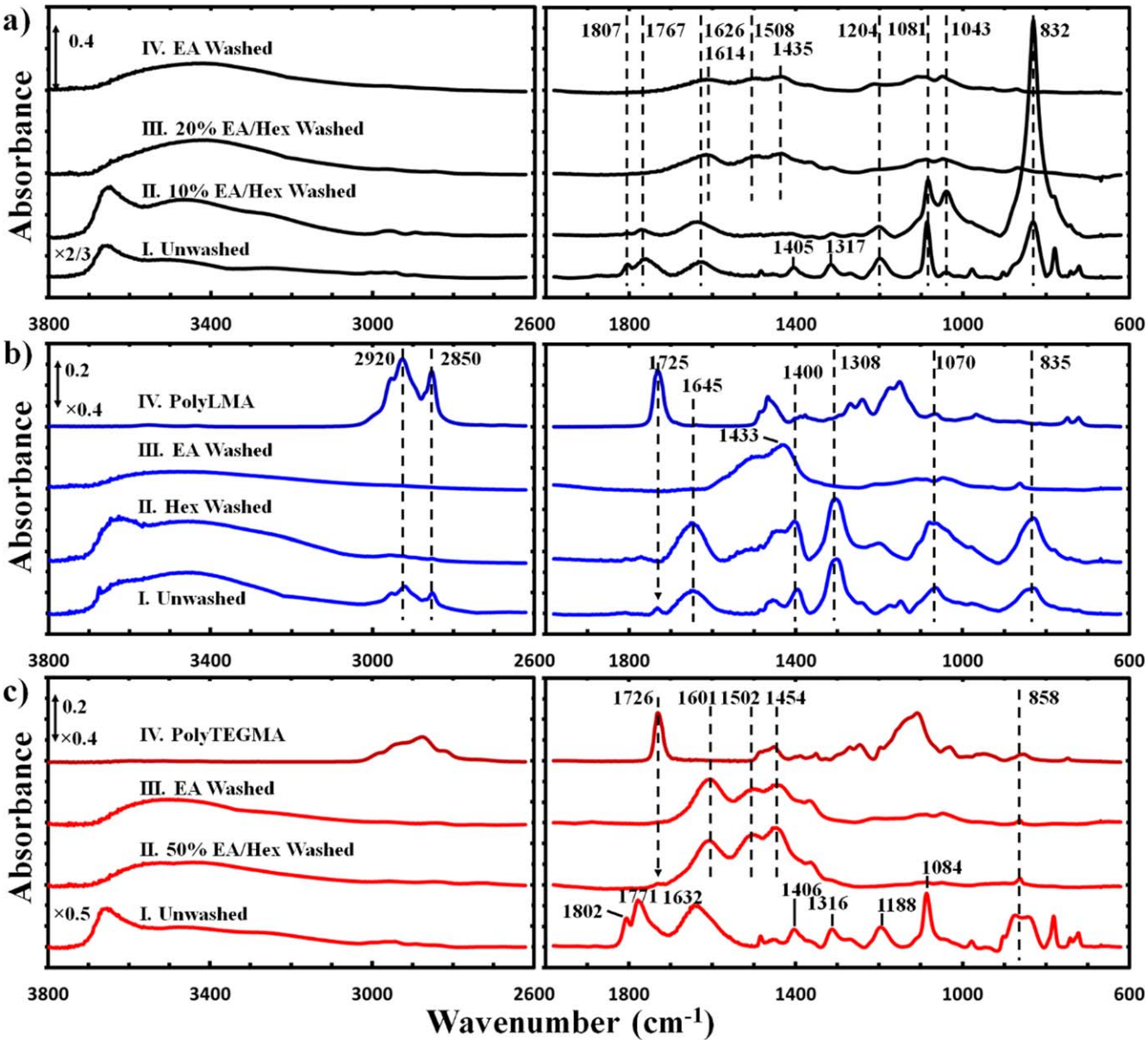

Figure 5. Selected FTIR spectra of unwashed and washed Si electrodes cycled with (a) no additive, (b) LMA additive and (c) TEGMA additive.

methacrylate additives could undergo polymerization to form protective SEIs. Slow scan rate was needed for formation of poly-LMA while the polymerization of TEGMA was tolerant of all tested conditions. The difference in their behaviors was due to their opposite polarities of molecular structures.

Gradient wash played a crucial role in sequential extraction of different components from the electrode surface to reveal the SEI and near SEI compositions by FTIR. The removal of residue electrolyte species by gradient wash has proven to be a consistent, polarity-controlled process. The sequential removal of different species assisted FTIR analysis as it revealed the internal correlations of the FTIR signals. This rationally controlled washing strategy was successfully applied to both Cu and Si electrodes, endorsing its universality for fractionating SEI components with molecular structure bias. It is worth noting that selective removal of targeted species such as electrolyte molecules can be readily achieved with gradient wash technique. It was also discovered that the chemistry of SEI formation is dependent on the reaction rate, where lower lithiation rate favors the formation of stabilizing lithium salts on the electrode surfaces, validating the slow charge formation processes widely used in industry.

Acknowledgments

This work was funded by the Assistant Secretary for Energy Efficiency, Vehicle Technologies Office of the US Department of Energy (US DOE) under the Si Consortium Program. Oak Ridge National Laboratory supplied silicon-coated copper electrodes. Some of the initial work on FTIR method development was performed at Molecular Foundry. Molecular Foundry was supported by the Office of Science, Office of Basic Energy Sciences, of the US Department of Energy under Contract No. DE-AC02–05CH11231.

References

1. J. R. Szczech and S. Jin, *Energy Environ. Sci.*, **4**, 56 (2011).
2. M. T. McDowell, S. W. Lee, W. D. Nix, and Y. Cui, *Adv. Mater.*, **25**, 4966 (2013).
3. K. Xu, *Chem. Rev.*, **114**, 11503 (2014).
4. X. Yu and A. Manthiram, *Energy Environ. Sci.*, **11**, 527 (2018).
5. K. Xu and A. von Cresce, *J. Mater. Chem.*, **21**, 9849 (2011).

6. K. Xu, *Chem. Rev.*, **104**, 4303 (2004).
7. L. Chen, K. Wang, X. Xie, and J. Xie, *J. Power Sources*, **174**, 538 (2007).
8. N.-S. Choi, K. H. Yew, K. Y. Lee, M. Sung, H. Kim, and S.-S. Kim, *J. Power Sources*, **161**, 1254 (2006).
9. C. C. Nguyen and B. L. Lucht, *J. Electrochem. Soc.*, **161**, A1933 (2014).
10. Y.-G. Ryu, S. Lee, S. Mah, D. J. Lee, K. Kwon, S. Hwang, and S. Doo, *J. Electrochem. Soc.*, **155**, A583 (2008).
11. Y. Li, G. Xu, Y. Yao, L. Xue, S. Zhang, Y. Lu, O. Toprakci, and X. Zhang, *J. Solid State Electrochem.*, **17**, 1393 (2013).
12. G.-B. Han, J.-N. Lee, J. W. Choi, and J.-K. Park, *Electrochim. Acta*, **56**, 8997 (2011).
13. S. J. Lee, J.-G. Han, Y. Lee, M.-H. Jeong, W. C. Shin, M. Ue, and N.-S. Choi, *Electrochim. Acta*, **137**, 1 (2014).
14. B. Philippe, R. Dedryvère, J. Allouche, F. Lindgren, M. Gorgoi, H. Rensmo, D. Gonbeau, and K. Edström, *Chem. Mater.*, **24**, 1107 (2012).
15. G. M. Veith, M. Doucet, J. K. Baldwin, R. L. Sacci, T. M. Fears, Y. Wang, and J. F. Browning, *J. Phys. Chem. C*, **119**, 20339 (2015).
16. M. Lu, H. Cheng, and Y. Yang, *Electrochim. Acta*, **53**, 3539 (2008).
17. L. Yang, B. Ravdel, and B. L. Lucht, *Electrochem. Solid-State Lett.*, **13**, A95 (2010).
18. L. J. Hardwick, M. Marcinek, L. Beer, J. B. Kerr, and R. Kostecki, *J. Electrochem. Soc.*, **155**, A442 (2008).
19. D. S. Hall, U. Werner-Zwanziger, and J. R. Dahn, *J. Electrochem. Soc.*, **164**, A2171 (2017).
20. R. Dedryvère, S. Laruelle, S. Grugeon, L. Gireaud, J.-M. Tarascon, and D. Gonbeau, *J. Electrochem. Soc.*, **152**, A689 (2005).
21. A. L. Michan, M. Leskes, and C. P. Grey, *Chem. Mater.*, **28**, 385 (2016).
22. A. V. Cresce, S. M. Russell, D. R. Baker, K. J. Gaskell, and K. Xu, *Nano Lett.*, **14**, 1405 (2014).
23. G. V. Zhuang, H. Yang, B. Blizanac, and P. N. Ross, *Electrochem. Solid-State Lett.*, **8**, A441 (2005).
24. A. Xiao, L. Yang, B. L. Lucht, S.-H. Kang, and D. P. Abraham, *J. Electrochem. Soc.*, **156**, A318 (2009).
25. L. Somerville, J. Bareño, P. Jennings, A. McGordon, C. Lyness, and I. Bloom, *Electrochim. Acta*, **206**, 70 (2016).
26. T. M. Fears, M. Doucet, J. F. Browning, J. K. S. Baldwin, J. G. Winiarz, H. Kaiser, H. Taub, R. L. Sacci, and G. M. Veith, *PCCP*, **18**, 13927 (2016).
27. G. V. Zhuang, K. Xu, H. Yang, T. R. Jow, and P. N. Ross, *J. Phys. Chem. B*, **109**, 17567 (2005).
28. Z. Li, C. Fang, C. Qian, S. Zhou, X. Song, M. Ling, C. Liang, and G. Liu, *ACS Applied Polymer Materials*, **1**, 1965 (2019).
29. C. Fang, G. Zhang, J. Lau, and G. Liu, *APL Mater.*, **7**, 080902 (2019).
30. M. Nie, D. P. Abraham, Y. Chen, A. Bose, and B. L. Lucht, *J. Phys. Chem. C*, **117**, 13403 (2013).
31. J. Yang, N. Solomatin, A. Kraytsberg, and Y. Ein-Eli, *ChemistrySelect*, **1**, 572 (2016).
32. S. Bhattacharya, A. R. Riahi, and A. T. Alpas, *Carbon*, **77**, 99 (2014).
33. P. Lanz and P. Novák, *J. Electrochem. Soc.*, **161**, A1555 (2014).
34. Y. Lai, Z. Cao, H. Song, Z. Zhang, X. Chen, H. Lu, M. Jia, and J. Li, *J. Electrochem. Soc.*, **159**, A1961 (2012).
35. M. L. Lazar and B. L. Lucht, *J. Electrochem. Soc.*, **162**, A928 (2015).
36. D. Chalasani, J. Li, N. M. Jackson, M. Payne, and B. L. Lucht, *J. Power Sources*, **208**, 67 (2012).
37. M. Nie, D. Chalasani, D. P. Abraham, Y. Chen, A. Bose, and B. L. Lucht, *J. Phys. Chem. C*, **117**, 1257 (2013).
38. K. Hongyou, T. Hattori, Y. Nagai, T. Tanaka, H. Nii, and K. Shoda, *J. Power Sources*, **243**, 72 (2013).
39. F. Shi, P. N. Ross, H. Zhao, G. Liu, G. A. Somorjai, and K. Komvopoulos, *J. Am. Chem. Soc.*, **137**, 3181 (2015).
40. H. Yang, G. V. Zhuang, and P. N. Ross, *J. Power Sources*, **161**, 573 (2006).
41. S. A. Freunberger, Y. Chen, Z. Peng, J. M. Griffin, L. J. Hardwick, F. Bardé, P. Novák, and P. G. Bruce, *J. Am. Chem. Soc.*, **133**, 8040 (2011).
42. L. Wang et al., *Nat. Chem.*, **11**, 789 (2019).
43. G. V. Zhuang and P. N. Ross, *Electrochem. Solid-State Lett.*, **6**, A136 (2003).
44. F. Shi, H. Zhao, G. Liu, P. N. Ross, G. A. Somorjai, and K. Komvopoulos, *J. Phys. Chem. C*, **118**, 14732 (2014).
45. C. Frangville, M. Hamel, G. H. V. Bertrand, E. Montbarbon, A. Grabowski, and C. Lynde, *Mater. Chem. Front.*, **3**, 1626 (2019).
46. W.-C. Kang, H.-G. Park, K.-C. Kim, and S.-W. Ryu, *Electrochim. Acta*, **54**, 4540 (2009).
47. C. C. Nguyen, H. Choi, and S.-W. Song, *J. Electrochem. Soc.*, **160**, A906 (2013).
48. C. C. Nguyen and S.-W. Song, *Electrochim. Acta*, **55**, 3026 (2010).